AAPS PharmSciTech, Vol. 11, No. 2, June 2010 (© 2010)
DOI: 10.1208/s12249-010-9436-6

Research Article

Physical Characterization of 1,3-dipropyl-8-cyclopentylxanthine (CPX)

Timothy McPherson,[1,4] Rahul V. Manek,[2] William Kolling,[1] Sihui Long,[3] and Tonglei Li[3]

Received 28 May 2009; accepted 16 April 2010; published online 4 May 2010

Abstract. 1,3-dipropyl-8-cyclopentylxanthine (CPX) has been shown to stimulate *in vitro* CFTR activity in ΔF508 cells. Data from a phase I study demonstrated erratic bioavailability and no measurable clinical response to oral CPX. One cause for its poor bioavailability may have been dissolution rate limited absorption, but there is little published physicochemical data on which to base an analysis. The objective of this study was to determine the solubility and solid-state characteristics of CPX. CPX is a weak acid with pKa of 9.83 and water solubility at pH7.0 of 15.6 μM. Both laureth-23 and poloxamer 407 increased the apparent water solubility linearly with increasing concentrations. CPX exists in two crystal forms, one of which (form II) has been solved. Form II is a triclinic crystal with space group P1 and calculated density of 1.278 g/cm^3. X-ray powder diffraction and differential scanning calorimetry studies (DSC) indicated that CPX crystals prepared at room temperature were mixtures of forms I and II. DSC results indicated a melting point of approximately 195°C for form I and 198°C for form II. Thermogravimetric analysis indicated no solvent loss upon heating. Dynamic water vapor sorption data indicated no significant water uptake by CPX up to 90% RH. Analysis of the data indicates that CPX may not be amenable to traditional formulation approaches for oral delivery.

KEY WORDS: CPX; pH solubility profile; physico-chemical characterization; thermal analysis; X-ray crystal structure.

INTRODUCTION

Cystic fibrosis (CF) is a genetic disorder caused by a mutation in the cystic fibrosis transmembrane conductance regulator (CFTR), a cell surface chloride (Cl^-) transporter. CFTR is expressed in epithelial cells that line the respiratory tract and pancreatic ducts, among other tissues (1,2). Mutation of the CFTR gene results in expression of lower than normal amounts of CFTR, non-functional CFTR, or both. These mutations significantly decrease the ability of exocrine epithelial cells to efflux Cl^- and water, resulting in excessively viscous secretions.

Deletion of phenylalanine at position 508 (ΔF508), the most common mutation responsible for CF, impairs trafficking of the CFTR protein to the cell membrane (3,4). 1,3-dipropyl-8-cyclopentylxanthine (CPX) has been shown to stimulate CFTR activity in ΔF508 cells by binding to the first nucleotide binding fold domain of the mutant CFTR protein in cell membranes (5–9). A patent on the use of CPX to treat CF was issued to the US government in 1994, and CPX was designated an orphan drug by the Food and Drug Administration in 1997 (10,11). In a phase I study of adult patients with mild CF, CPX exhibited erratic bioavailability and no indication of short-term clinical effectiveness (12).

CPX (Fig. 1) is a weak acid structurally similar to theophylline and caffeine. There is little published data on the physical properties of CPX. Advanced Chemistry Development software (ACD Labs, V8.14) predicts CPX log P= 3.379±0.429, pK_a=9.29±0.70, and water solubility=55 μM at pH7 (13). While details on the dosage forms used in the clinical studies are unavailable, it is plausible that the erratic bioavailability and lack of effectiveness were due, in part, to dissolution rate-limited absorption.

Since it has been estimated that only 5% of normal CFTR activity is sufficient to maintain a normal cellular phenotype, there is great potential for drugs such as CPX to improve the quality of life for CF patients (2). The objective of this study was to determine the solubility and solid-state characteristics of CPX. Solubility data and the characterization of solid-state forms may serve as a guide for potential improvements in CPX bioavailability.

MATERIALS AND METHODS

SciClone Pharmaceuticals (Foster City, CA, USA) provided a sample of CPX for solubility determinations. CPX for all other analyses was synthesized using a minor modification of published methods (14–17). The structure of synthesized CPX was confirmed by NMR (not shown) and X-ray crystallography (below). The purity was greater than 99% as determined by HPLC/MS.

[1] Department of Pharmaceutical Sciences, Southern Illinois University Edwardsville School of Pharmacy, Edwardsville, Illinois 62026, USA.
[2] Exelixis Inc., South San Francisco, California, USA.
[3] Pharmaceutical Sciences, University of Kentucky College of Pharmacy, Lexington, Kentucky, USA.
[4] To whom correspondence should be addressed. (e-mail: tmcpher@siue.edu)

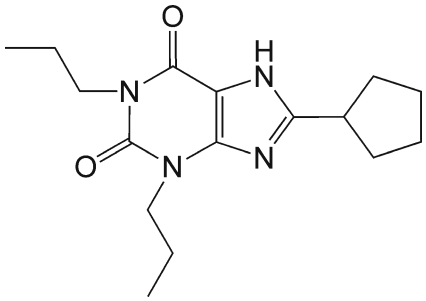

Fig. 1. CPX chemical structure

Equilibrium Solubility Measurement

The general procedure for equilibrium solubility measurements was as follows. Approximately 50 mg of CPX was weighed into Erlenmeyer flasks and wetted with 100 μl of ethanol then diluted with 40 ml of buffer solution. The mixture was shaken on a platform shaker at room temperature for up to 72 h. Samples for analysis were withdrawn at approximately 24-h intervals and filtered through a 0.45 μm nylon filter. Mixtures were defined to have reached equilibrium when two consecutive measurements agreed within 5%.

The dissolved CPX concentration was assayed by UV absorption at 277 nm with a Cary 50 spectrophotometer. The concentration was quantified by comparison to a standard Beer's Law plot. CPX solubility was measured at pH7.0 in 100 mM phosphate buffer, pH8.0 and 9.0 in 100 mM Tris buffer, and pH10.0 and 11.0 in 100 mM glycine buffer. The buffer solutions did not interfere with the UV analysis. The pK_a for the acidic N-H functionality was estimated by fitting the solubility data to Eq. 1, utilizing KaleidaGraph 4.0.1. The software fitting routine was validated using published data sets. S_t is the solubility at a given proton molar concentration, S_0 is the intrinsic solubility, and K_a is the acid dissociation constant (18).

$$S_t = S_0\left(1 + \frac{K_a}{[H^+]}\right) \quad (1)$$

The effects of solubilizing agents on CPX apparent water solubility was similarly determined in pH7.0 buffer containing either laureth-23 (polyoxyl 23 lauryl ether, Brij® 35; 0.1%, 0.5%, and 1.0%) or poloxamer 407 (0.5%, 1.0%, or 2.5%). The appropriate buffer solution served as the blank for all measurements.

Polymorph Screening

CPX was recrystallized from water and several organic solvents to search for polymorphic forms. Samples were obtained from acetone, methanol, 95% ethanol, isopropanol, and ethyl acetate by slow evaporation of the solvent to dryness at room temperature. Slow evaporation, achieved by covering the beaker with plastic film that was perforated with several small holes, was typically complete within 48 h. Methanol was also used to recrystallize CPX by slow cooling of a supersaturated solution and by fast evaporation to dryness at room temperature. Fast evaporation, achieved by leaving the solution uncovered, was complete in less than 24 h. Recrystallization from dimethylsulfoxide was accomplished by slow cooling of a saturated solution. Finally, CPX was recrystallized from water by adjusting an alkaline CPX solution (pH12) with concentrated HCl to pH7. The solid was collected by vacuum filtration, washed with several aliquots of water, and dried under vacuum at room temperature.

Thermal Analysis

The thermal behavior of CPX samples was determined on a TA Instruments Q100 differential scanning calorimeter (DSC). The cell constant was determined using the recommended indium calibration procedure. Samples (approximately 1-2 mg) were analyzed under dry nitrogen flow at 50 ml/min in sealed aluminum pans. The heating and cooling rate for all analyses was 10°C/min.

Thermogravimetric analysis (TGA) was performed with a TA Instruments TGA Q500 with a 16 position autosampler. The microbalance was periodically calibrated using certified calcium oxalate. Typically 2-10 mg of the sample was loaded onto a platinum crucible. Samples were analyzed from ambient to 250°C at a heating rate of 10°C/min under a continuous nitrogen flow of 50 mL/min. DSC and TGA data were analyzed using the TA Universal Analysis software.

Single Crystal X-Ray Diffraction

Samples for single-crystal X-ray diffraction (SXRD) were prepared by a sublimation method. Approximately 5 mg of CPX was heated on a microscope slide at 180°C on an Instec HCS302 hot-stage with an Instec STC200 heating system overnight. Crystals formed on the cover slip and were collected for analysis. Data collection was carried out at –183°C on a Bruker X8 Proteum Diffractometer with Cu Kα radiation (1.54178 Å). Cell refinement and data reduction were conducted with SCALEPACK and DENZO-SMN (19). Structure solution and refinement were completed with SHELXS97 and SHELXL97, respectively (20,21). Mercury software (v1.4.2, Cambridge Crystallographic Data Centre) was used to generate the predicted X-ray powder diffraction pattern for comparison with experimental data.

X-ray Powder Diffraction

X-ray powder diffraction (XRPD) data were collected using a Rigaku Miniflex+(Rigaku Americas) with SC-M scintillation counter detector. Scans were obtained from 5° to 25° 2θ with steps of 0.03° and scan rate of 1.5°/min. All samples were ground with an agate mortar and pestle prior to analysis. The powders were analyzed on a Si zero-background sample holder. The samples were illuminated using Cu Kα radiation at 30 kV and 15 mA while being rotated to minimize effects of preferred orientation. A nickel filter was used to reduce the Kβ contribution to the X-ray signal.

Dynamic Water Vapor Sorption

Moisture sorption isotherms were generated at 25°C using a DVS Advantage 1 (Surface Measurement Systems) equipped with a Cahn electronic microbalance and a dew point analyzer for the accurate measurement of weight and

relative humidity (RH), respectively. Samples were first dried at 0% RH and 45°C. Sorption and desorption curves were generated in 10% steps from 10% to 90% RH. Equilibrium was defined as a sample weight change of 0.002% or less over a period of 5 min. Maximum equilibration time was set at 3 h per step. The instrument was periodically calibrated using saturated salt solutions for RH and certified weights for the microbalance. Data was analyzed using the DVS Advantage Analysis Suite.

RESULTS

Equilibrium Solubility Measurement

The CPX powder did not disperse in water even with vigorous mixing or brief intermittent sonication. The hydrophobic particles floated on the surface of the water and adhered to the container. Wetting the powder with 100 µl of alcohol prior to adding the aqueous dissolution medium resulted in dispersion of the particles and reproducible solubility data.

The effect of pH on CPX water solubility (mean± standard deviation, n=3) is shown in Fig. 2. CPX solubility increased from 15.6 µM at pH7-253.2 µM at pH 11. Fitting Eq. 1 to the data resulted in correlation coefficient (r^2) of 0.99991 with S_0=15.888 µM and K_a=1.493×10^{-10} (pK_a=9.83). Laureth-23 and poloxamer 407 solubilized CPX at the higher concentrations (Fig. 3), but not at the lowest surfactant concentrations studied. Both laureth-23 and poloxamer 407 increased CPX apparent water solubility linearly with surfactant concentration (r^2=0.9999 and 0.9919, respectively).

Polymorph Screening

CPX produced fine acicular crystals from all organic solvents tested. Crystals from the different solvents were visually indistinguishable when viewed with a light microscope (Leica DM IRE2). The delicate crystals were prone to splitting parallel to their long axes when manipulated. DSC and XRPD analyses (below) indicated that all of the CPX samples from organic solvents were equivalent. The crystals obtained from organic solvents at room temperature were not suitable for SXRD analysis. CPX crystals for SXRD analysis were instead prepared by sublimation. CPX obtained by precipitation from aqueous solution was a fine white powder, visually distinguishable from the acicular crystals obtained from the organic solvents.

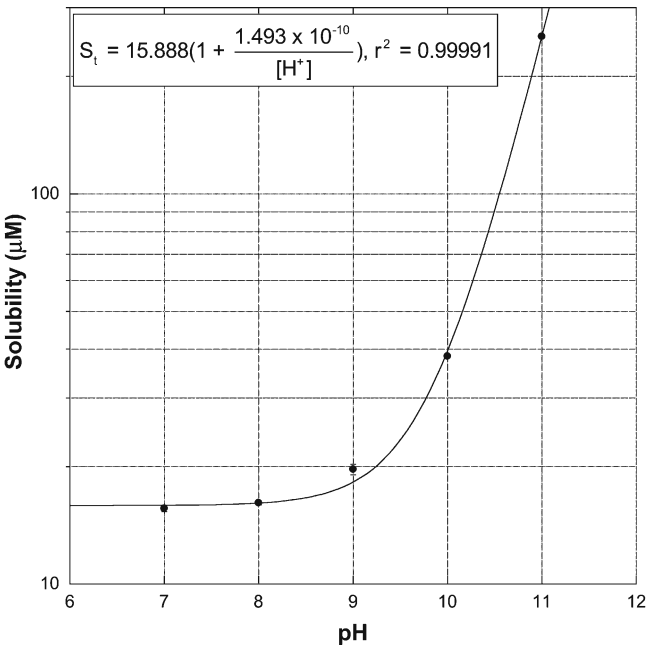

Fig. 2. CPX solubility as a function of pH

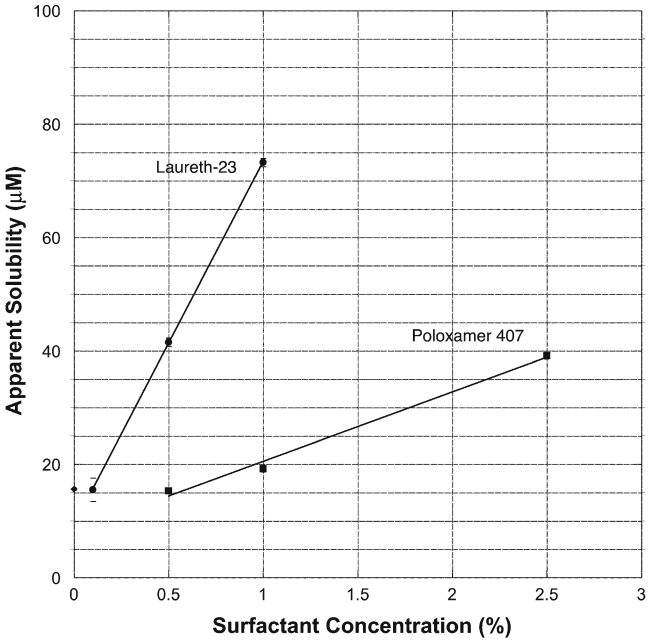

Fig. 3. CPX apparent water solubility at pH7 as a function of solubilizing agent concentration

Thermal Analysis

CPX crystals obtained from all organic solvents exhibited equivalent DSC thermograms, while CPX obtained by precipitation from water was qualitatively different. Therefore, only data for CPX obtained by fast evaporation of methanol and by precipitation from water are presented. All replicate samples were highly reproducible. No thermograms showed thermal events below 190°C, nor was there evidence of glass transitions, desolvation, or degradation below the melting temperature. The heating and cooling rates for all DSC experiments were 10°C/min.

Figure 4 shows the DSC thermograms for CPX crystals obtained from methanol. Curve A in Fig. 4 represents the thermogram obtained by heating a sample to 210°C. Two thermal events are evident, with peak temperatures of 195.0°C and 197.8°C. Curve B in Fig. 4 shows the thermogram when the sample in Curve A in Fig. 4 is cooled to 40°C, then heated again to 210°C. This second heating cycle similarly shows two thermal events. Curve C in Fig. 4 represents the second heating cycle of a fresh CPX sample that has first been heated to 196°C, cooled to 40°C, then heated to 210°C. Curve C in Fig. 4 shows only one thermal event with a sharp peak with onset temperature of 195.9°C, peak temperature 197.7°C, and heat of fusion (ΔH_f) of 92.7 J/g.

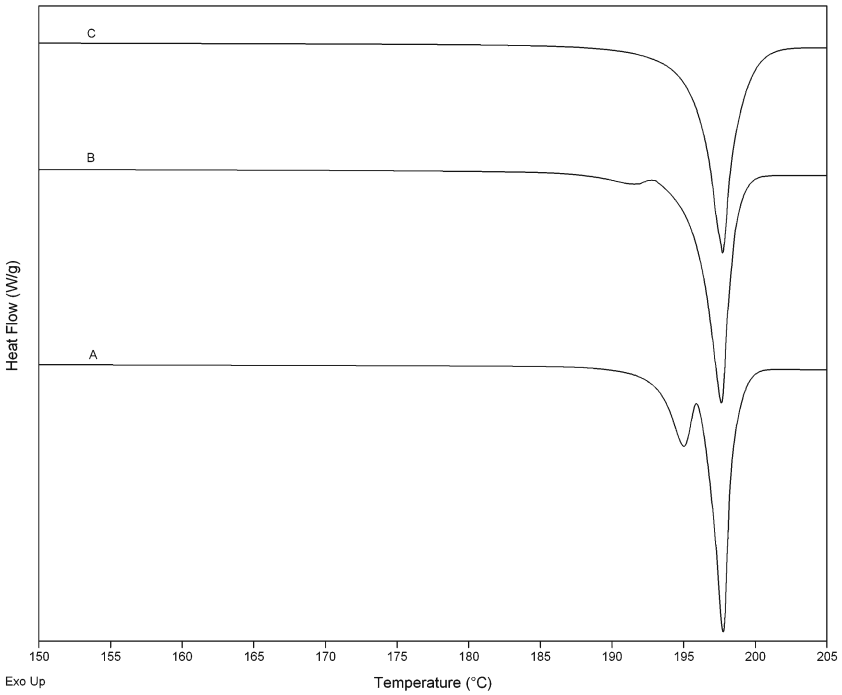

Fig. 4. DSC thermograms for CPX obtained from methanol. CPX sample heated to 210°C (*a*), CPX heated to 210°C, cooled to 40°C, then heated again to 210°C (*b*), CPX heated to 196°C, cooled to 40°C, then heated to 210°C (*c*)

Figure 5 shows the thermograms for CPX obtained by precipitation from water. Curve A in Fig. 5 represents the thermogram obtained by heating the sample to 210°C. This curve exhibits two thermal events. There is one obvious peak at 198.3°C that is preceded by a shoulder, or region of sharper slope, in the range of 191–195°C. Curve B in Fig. 5 shows the thermogram when the sample in Curve A in Fig. 5 is cooled from 210°C to 40°C, then heated again to 210°C. There are clearly two thermal events in this curve, with peak temperatures of 195.3°C and 198.0°C. Curve 5C represents the second heating cycle of a fresh CPX sample that has first been heated to 196°C, cooled to 40°C, then heated again to 210°C. Similar to

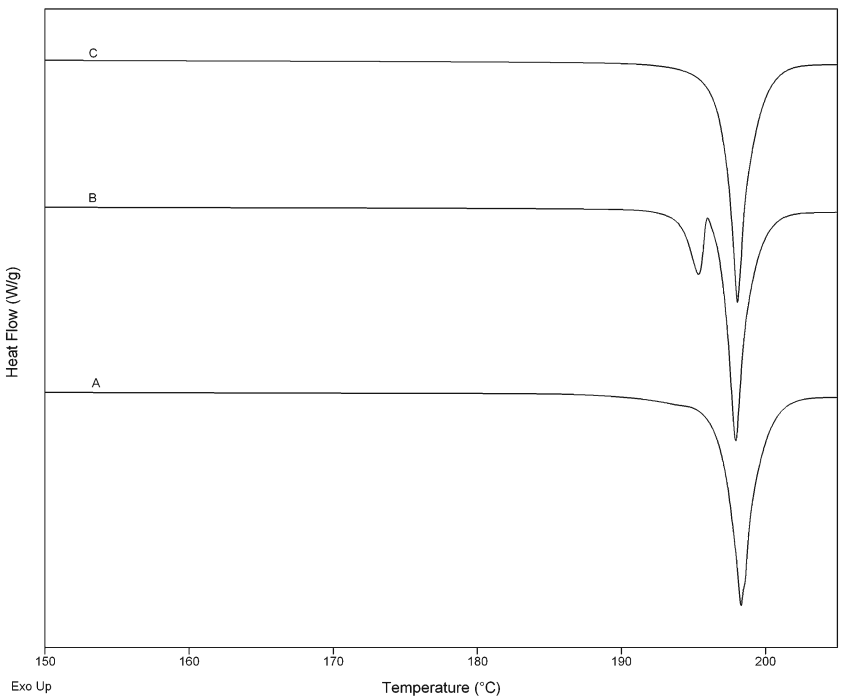

Fig. 5. DSC thermograms for CPX obtained from water. CPX sample heated to 210°C (*a*), CPX heated to 210°C, cooled to 40°C, then heated again to 210°C (*b*), CPX heated to 196°C, cooled to 40°C, then heated to 210°C (*c*)

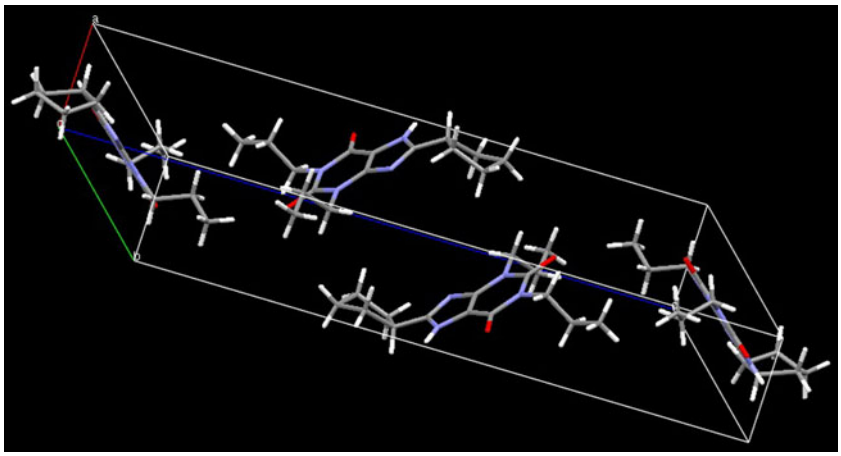

Fig. 6. Crystal structure for CPX form II

Curve C in Fig. 4, there is a single peak with onset temperature of 197.0°C, peak temperature of 198.0°C, and ΔH_f of 91.1 J/g.

TGA showed that CPX from methanol exhibited weight loss of 0.18% at 150°C. Weight loss increased to approximately 0.75% as the temperature approached 200°C. The aqueous CPX precipitate similarly showed weight loss of 0.2% at 150°C.

Single Crystal X-Ray Diffraction

The largest crystals obtained by sublimation (about 0.25×0.02×0.02 mm) were submitted for structure determination. The unit cell is shown in Fig. 6 and experimental details are summarized in Table I. SXRD confirmed the structure of CPX synthesized in our laboratory. The xanthine ring system is essentially planar, as expected. The n-propyl and cyclopentyl substituents are extended and oriented away from the xanthine ring system in a *trans*-like conformation. The relatively large R1 value, 0.1076, can be attributed to the small crystal size.

X-ray Powder Diffraction

Figure 7 shows the experimental powder X-ray diffractograms for CPX obtained from methanol (a in Fig. 7) and water (b in Fig. 7) and the predicted diffractogram (p in Fig. 7) calculated from the single crystal structure. CPX obtained from methanol shows several major peaks between 5° and 25° 2θ. The peaks are sharp and well defined. Most of the peaks align with the predicted pattern with the exception of those at 6.2°, 9.5°, and 12.5° 2θ. The aqueous precipitate exhibits fewer peaks, most of which are poorly formed. There is no indication of amorphous halos in either of the experimental diffractograms. All of the peaks in the aqueous CPX sample coincide with peaks in the methanol CPX sample.

Table I. CPX Crystal Data and Structure Refinement

Empirical formula	$C_{16}H_{24}N_4O_2$
Formula weight	304.39
Temperature	−183°C
Wavelength	1.54178 Å
Crystal system	Triclinic
Space group	P1
Unit cell dimensions	a= 4.6481(4), b=14.0540(13), c=25.250(2) Å α=73.986(5), β=89.178(8), γ=86.570(7)°
Z	4
Crystal density (calculated)	1.278 g/cm^3
R1	0.1076

Figure 8 shows the diffractograms for CPX samples that were heated in the DSC to 210°C and cooled to room temperature. Both the methanol (a in Fig. 8) and water (b in Fig. 8) samples show several sharp peaks. With the exception of the peaks at 6.2°, 9.5°, and 12.5° 2θ, all of the peaks in the experimental diffractograms are represented in the predicted pattern. The experimental diffractograms appear to be equivalent to each other and substantially similar to the predicted pattern.

Figure 9 shows the diffractograms for CPX samples that were heated in the DSC to 196°C then cooled to room temperature. The methanol (a in Fig. 9) and water (b in Fig. 9) samples both exhibit many sharp peaks and appear substantially equivalent to each other. All of the peaks in both experimental diffractograms align with corresponding peaks in the predicted pattern (p in Fig. 9). Both diffractograms are substantially equivalent to the predicted pattern, and neither exhibits peaks at 6.2°, 9.5°, or 12.5° 2θ.

Dynamic Water Vapor Sorption

CPX did not take up water in the relative humidity range of 10-90% at 25°C. Sample weight change remained less than 0.1% at all points in both the adsorption and desorption phases. There was no indication of any physical change in the material throughout the process.

DISCUSSION

The Biopharmaceutics Classification System (BCS) is used to classify drugs according to water solubility and intestinal permeability parameters (22). CPX is a low solubility drug as more than 250 ml would be required to dissolve any dose greater than 1.2 mg. In the absence of human *in vivo* data, the cLogP value of 3.379±0.429 would

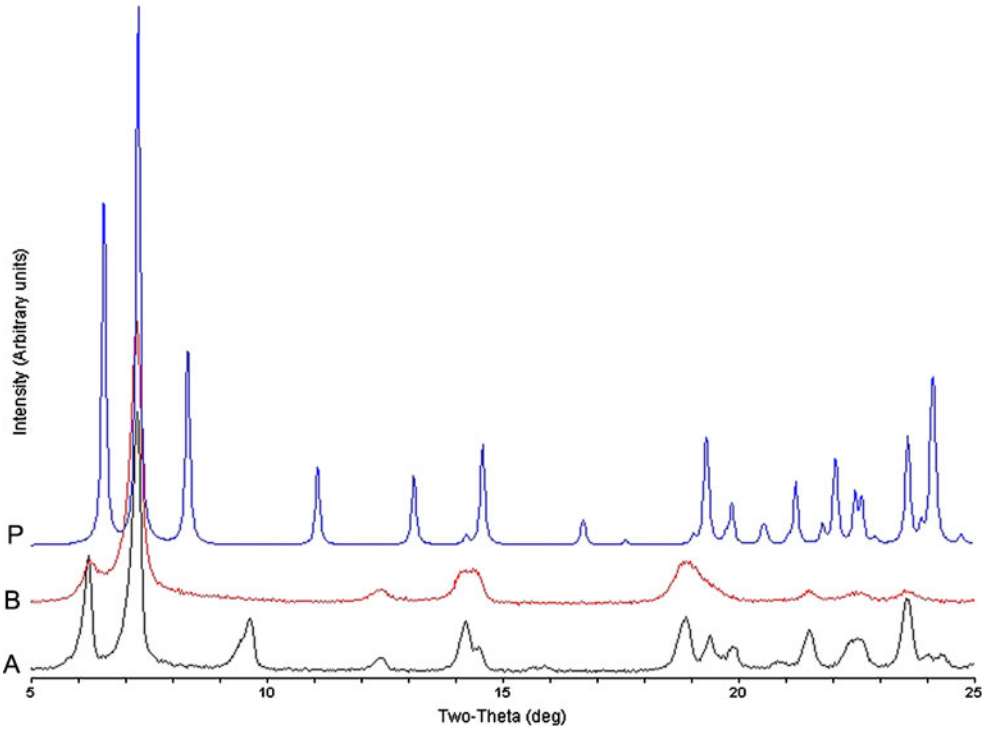

Fig. 7. X-ray powder diffractograms for CPX obtained from methanol (*a*) and water (*b*) and the diffractogram for form II predicted from the single crystal structure (*p*)

classify CPX as a high intestinal permeability drug (13,23,24). Thus, CPX would be assigned to BCS Class II (low solubility and high permeability). Applying the analysis described by Gu *et al.* for highly permeable drugs, the maximum absorbable oral dose of CPX is approximately 3 mg (24). Thus, the finding of unpredictable oral absorption of CPX in parallel cohorts of four or five CF patients is not surprising (12).

Absorption of class II drugs may be enhanced by delivery systems that maximize the *in vivo* solubility and dissolution rate and by administering the drug with a high fat

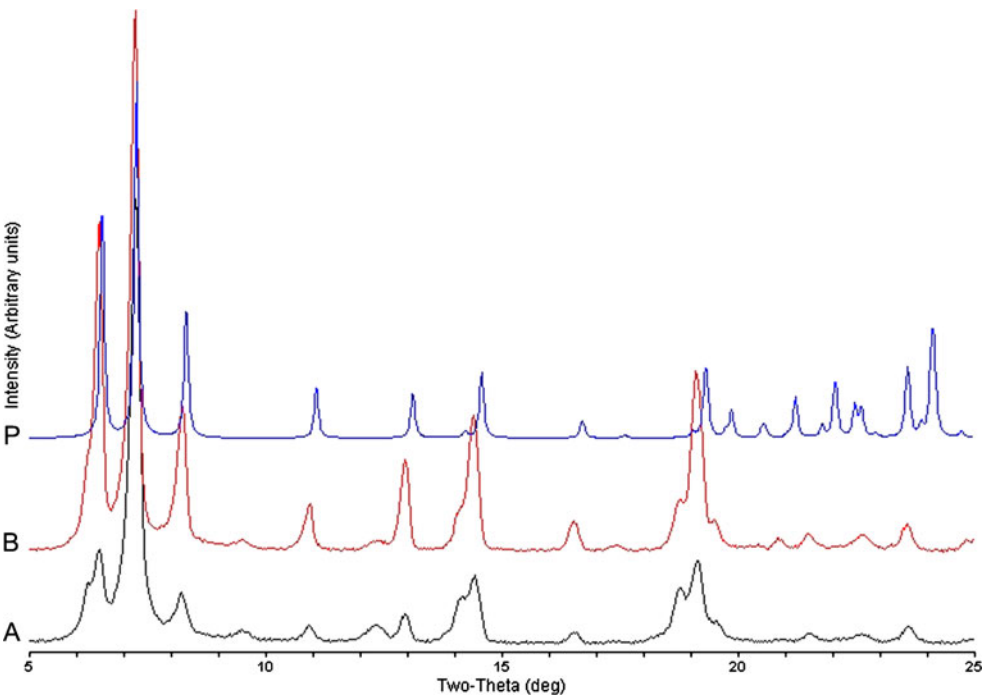

Fig. 8. X-ray powder diffractograms for CPX obtained from methanol (*a*) and water (*b*) after heating to 210°C then cooling to room temperature and the diffractogram for form II predicted from the single crystal structure (*p*)

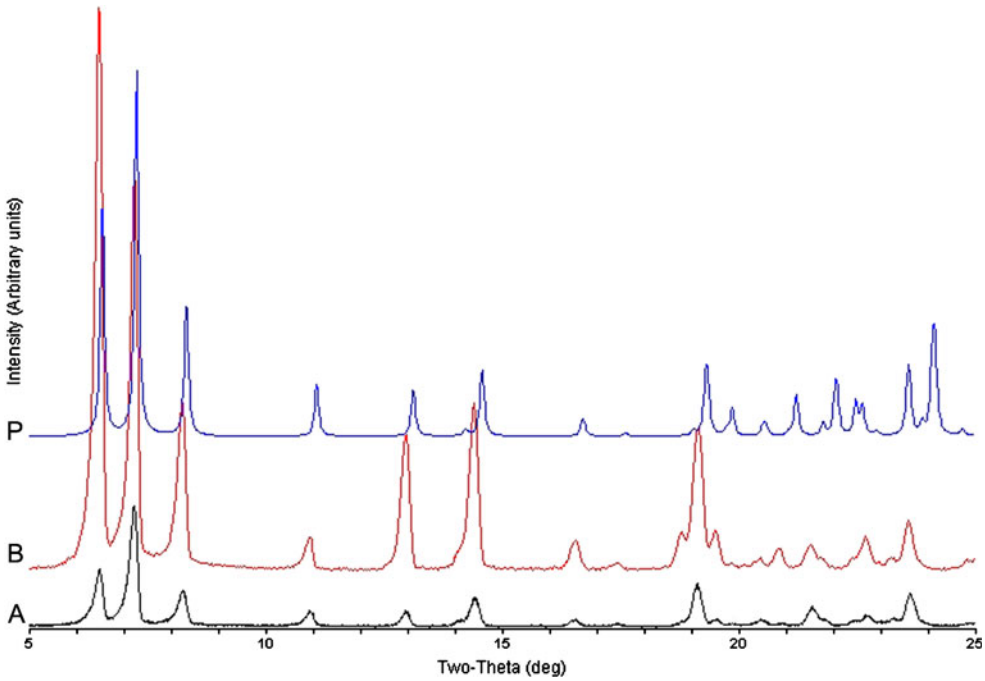

Fig. 9. X-ray powder diffractograms for CPX obtained from methanol (*a*) and water (*b*) after heating to 196°C then cooling to room temperature and the diffractogram for form II predicted from the single crystal structure (*p*)

meal (24–27). Rudolph and Tuthill claimed improved absorption of CPX delivered as a suspension in corn oil as compared to a gelatin capsule (28). Average C_{max} for a 300 mg dose was approximately 675 ng/ml (n=3) for the corn oil suspension and approximately 150 ng/ml for the gelatin capsule (n=4). As a comparison, McCarty reported an average C_{max} of 250 ng/ml for a 300 mg oral dose in four CF patients (12). Absorption enhancement by corn oil may be partially related to improved wetting, as CPX powder dispersion in water was found to be poor.

CPX solubility increased with pH, as expected for a weak acid. Due to its high pK_a, however, the pH elevation required to achieve a significant increase in CPX solubility is unreasonable for oral dosage forms. Attempts in our lab to prepare the salt forms of CPX have been unsuccessful. Micronization is useful only for drugs with slow dissolution unrelated to low solubility (18).

Drug solubility and dissolution rate may also be increased by including surfactant solubilizing agents in the formulation. Surfactants may function both to increase apparent water solubility of the drug and to promote wetting of solid particles in the aqueous GI fluid. The effects of two common surfactants on CPX apparent water solubility were studied. Laureth-23 and poloxamer 407 both enhanced CPX apparent solubility up to fivefold. This apparent solubility would increase the maximum absorbable dose of CPX to approximately 15 mg. Increasing surfactant concentrations to further increase drug solubility is possible, but may be limited by other considerations. For example, solution viscosity increases with poloxamer 407 concentration and the aqueous solutions gel at approximately 18%, resulting in counterproductive decrease in dissolution rate (29). High concentrations of surfactants may also be irritating or toxic to the GI mucosa.

Insoluble drugs may be formulated as soluble complexes to improve oral bioavailability. Theophylline forms soluble complexes with a variety of alkylamines, including ethylenediamine (30). Cyclodextrins are also commonly used to enhance absorption of a variety of drugs. Previous study indicated that CPX does not form soluble complexes with ethylenediamine, ethanolamine, or hydroxypropyl-β-cyclodextrin (31).

Solubility differences of multiple crystal or amorphous forms of a drug may be exploited for dissolution enhancement if they are sufficiently stable. DSC and XRPD data show no evidence of amorphous CPX, and the lack of significant weight loss on heating argues against a solvated form. However, XRPD and DSC analyses support the existence of at least two crystal forms of CPX, one of which has been solved by SXRD.

CPX was recrystallized from water and organic solvents at room temperature and *via* sublimation at 180°C. The sample prepared by sublimation represents a pure crystal form, denoted here as form II. Thermal analysis and XRPD data suggest that all samples produced at room temperature are mixtures of form II and another polymorph (form I) that has not been isolated in pure form. DSC thermograms of CPX obtained from methanol (Fig. 4a) and water (Fig. 5a) both show two thermal events at approximately 195° and 198°C. While the two peaks are obvious in Fig. 4a, close examination reveals that the first thermal event in Fig. 5a is represented as a shoulder preceding the peak. The event at 195°C represents melting of form I while the event at 198°C represents the melting of form II. The two peaks are not completely resolved in either thermogram, suggesting that melting of form I is incomplete when melting of form II begins.

The powder diffractograms corresponding to these samples (Fig. 7a and b, respectively) show many common

peaks. Both experimental diffractograms have some peaks in common with the predicted pattern for form II (Fig. 7p) and some peaks that are not found in the predicted pattern (6.2º, 9.5º, and 12.5º 2θ). The aqueous sample exhibits fewer peaks than the methanol sample, but all of the peaks in the aqueous sample are found in the methanol sample. Both experimental diffractograms are shifted to slightly lower 2θ values than the predicted pattern, as expected due to the fact that the SXRD data were collected at −183°C and the XRPD data were collected at room temperature (24°C; 32). Predicted XRPD patterns frequently contain more peaks than a corresponding experimental pattern of the same pure crystalline form, as they represent all possible peaks that may be expected from a material irrespective of sample preparation. The predicted pattern was calculated from the single crystal structure, which represents a pure form. That there are additional peaks in the experimental XRPD pattern suggests that at least one additional crystal form is present.

Melting either CPX sample to 210°C, cooling to 40°C, then heating again resulted in two obvious thermal events (Fig. 4b and 5b). The cause for the first peak shift to lower temperature in Fig. 4b is unknown and has not yet been investigated. This phenomenon is reproducible however. The powder diffractograms corresponding to these samples (Fig. 8a and b, respectively) are qualitatively identical. Both diffractograms exhibit a peak at 8.5º 2θ that was not found in Fig. 7a and b. Both Fig. 8a and b exhibit peaks at 6.2º, 9.5º and 12.5º 2θ, in addition to the peaks that are common to the predicted diffractogram for form II.

Heating to 196°C then cooling to 40°C resulted in a single melting peak at approximately 198°C for both the methanolic and aqueous CPX samples (Figs. 4c and 5c). The corresponding powder diffractograms (Fig. 9a and b) are qualitatively indistinguishable from each other. Further, all of the peaks in experimental diffractograms correspond to predicted peaks for form II.

Thus, it appears that all CPX samples produced at room temperature represent mixtures of form I and form II. The difference between samples obtained from water and methanol appears to be the proportion of the two crystal forms present. Based on DSC and XRPD, the aqueous sample contains a lower proportion of form I than the methanolic samples, but it cannot be considered as representing pure form II due to the thermal event at 195°C (Fig. 5a) and the XRPD peaks at 6.2º and 12.5º 2θ (Fig. 7b). CPX obtained from methanol appears to contain a greater proportion of form I, and DSC and XRPD corroborate the presence of a mixture in this sample also. Heating either sample to 196°C appears to convert the mixture to essentially pure form II. This conclusion is based on analysis of the DSC thermograms and XRPD diffractograms. Figures 4c and 5c exhibit a single melting endotherm at approximately 198°C. Figures 9a and b show that the XRPD diffractograms are qualitatively indistinguishable from each other and from the predicted diffractogram for form II. Heating to 196°C thus appears to result in melting of the form I crystals present in the sample, followed by crystallization as form II when the sample is cooled to 40°C.

The physical basis for the difference between CPX obtained from water and methanol may be related to the kinetics of crystallization. CPX crystallization from water was rapid as the solubility was decreased by the addition of HCl to an alkaline solution of CPX. Crystallization was complete within seconds of neutralization to pH7. CPX crystals obtained from methanol were formed in a relatively slow process, requiring at least several hours. Unfortunately, the inability to generate pure form I crystals precludes the precise quantitation of forms present in the mixtures generated at room temperature.

In summary, CPX is practically insoluble in the physiologically relevant pH range and does not appear to be amenable to oral delivery using traditional formulation approaches. Prodrugs or analogs of CPX with enhanced water solubility appear to be more likely to provide effective oral delivery.

CONCLUSION

The water solubility of CPX at pH7 is approximately 15.6 μM. Increasing pH or addition of surfactant solubilizing agents result in greater apparent water solubility. CPX appears to exist in two crystal forms, one of which has been isolated in pure form. CPX samples recrystallized at room temperature represent mixtures of the two crystal forms. Careful analysis of the data suggests that CPX may not be amenable to the traditional formulation approaches for effective oral delivery.

ACKNOWLEDGMENTS

The authors acknowledge SciClone Pharmaceuticals, Inc. for providing CPX for solubility experiments and Dr. A. Michael Crider for assistance with CPX synthesis. We acknowledge support *via* National Science Foundation grants DMR-0449633 (TL) and DUE-0410642 (SIUE).

REFERENCES

1. Gadsby DC, Vergani P, Csanady L. The ABC protein turned chloride channel whose failure causes cystic fibrosis. Nature. 2006;440:477–83.
2. Strasbaugh SD, Davis PB. Cystic fibrosis: a review of epidemiology and pathobiology. Clin Chest Med. 2007;28:279–88.
3. Registry P. Annual report. Bethesda, MD: Cystic Fibrosis Foundation; 2005. 2006.
4. Cheng SH, Gregory RJ, Marshall J, Paul S, Souza DW, White GA *et al*. Defective intracellular transport and processing of CFTR is the molecular basis of most cystic fibrosis. Cell. 1990;163:827–34.
5. Andersson C, Roomans G. Activation of deltaF508 CFTR in a cystic fibrosis respiratory epithelial cell line by 4-phenylbutyrate, genistein and CPX. Eur Respir J. 2000;15:937–41.
6. Cohen B, Lee G, Jacobson K, Kim Y, Huang Z, Sorscher E *et al*. 8-cyclopentyl-1, 3-dipropylxanthine and other xanthines differentially bind to the wild-type and delta F508 first nucleotide binding fold (NBF-1) domains of the cystic fibrosis transmembrane conductance regulator. Biochem. 1997;36:6455–61.
7. Eidelman O, Barnoy S, Razin M, Zhang J, Mcphie P, Lee G *et al*. Role for phospholipid interactions in the trafficking defect of Delta F508-CFTR. Biochem. 2002;41:11161–70.
8. Eidelman O, Guay-Broder C, Van Galen PJM, Jacobson KA, Fox C, Turner RJ *et al*. A1 adenosine-receptor antagonists activate chloride efflux from cystic fibrosis cells. Proc Natl Acad Sci USA. 1992;89:5562–6.
9. Jacobson KA, Guay-Broder C, Van Galen PJM, Gallo-Rodriguez C, Melman N, Jacobson MA *et al*. Stimulation by alkylxanthines of chloride efflux in CFPAC-1 cells does not involve A1 adenosine receptors. Biochem. 1995;34:9088–94.

10. US FDA: Cumulative list of all orphan designated products. www.fda.gov/orphan/designat/alldes.rtf. Accessed 24 Aug 2007.
11. Pollard HB, Van Galen PJM, Jacobson KA, inventors; United States of America as represented by the Department of Health and Human Service, assignee. Method of treating cystic fibrosis using 8-cyclopenty-1,3-dipropylxanthine or xanthine amino congeners. US patent 5,366,977. 1994 Nov 22.
12. McCarty NA, Standaert TA, Teresi M, Tuthill C, Launspach J, Kelly TJ *et al.* A phase I randomized, multicenter trial of CPX in adult subjects with mild cystic fibrosis. Pediatr Pulmonol. 2002;33:90–8.
13. SciFinder Scholar: Substance detail 102146-07-6. Accessed 19 Mar 2009.
14. Daly J, Padgett W, Shamim M, Butts-Lamb P, Waters J. 1, 3-Dialkyl-8-(p-sulfophenyl)xanthines: potent water-soluble antagonists for A1- and A2-adenosine receptors. J Med Chem. 1985;28:487–92.
15. Erickson R, Hiner R, Feeney S, Blake P, Rzeszotarski W, Hicks R *et al.* 1, 3, 8-trisubstituted xanthines. Effects of substitution pattern upon adenosine receptor A1/A2 affinity. J Med Chem. 1991;34:1431–5.
16. Scammells P, Baker S, Belardinelli L, Olsson R. Substituted 1, 3-dipropylxanthines as irreversible antagonists of A1 adenosine receptors. J Med Chem. 1994;37:2704–12.
17. Shamim MT, Ukena D, Padgett W, Hong O, Daly J. 8-Aryl-and 8-cycloalkyl-1, 3-dipropylxanthines: further potent and selective antagonists for A1-adenosine receptors. J Med Chem. 1988;31:613–7.
18. Martin A. Physical pharmacy. 4th ed. Baltimore, MD: Williams & Wilkins; 1993.
19. Otwinowski Z, Minor W. Processing of x-ray diffraction data collected in oscillation mode. In: Carter Jr CW, Sweet RM, editors. Macromolecular crystallography, Part A. New York: Academic; 1997. p. 307–26.
20. Sheldrick G. Shelxl97 and Shelxs97 [Computer Software]. Germany: University of Göttingen; 1997.
21. Sheldrick G. Shelxtl/PC [Computer Software]. Madison, WI: Siemens Analytical X-ray Instruments, Inc; 1995.
22. US FDA: Guidance for Industry: Waiver of *in vivo* bioavailabilty and bioequivalence studies for immediate-release solid oral dosage forms based on a biopharmaceutics classification system. http://www.dfa.gov/cder/guidance/index.htm Accessed 19 Mar 2009.
23. Benet L, Amidon G, Barends D, Lennernas H, Polli J, Shah V *et al.* The use of BDDCS in classifying the permeability of marketed drugs. Pharm Res. 2008;25:483–8.
24. Gu CH, Li H, Levons J, Lentz K, Gandhi R, Raghavan K *et al.* Predicting effect of food on extent of drug absorption based on physicochemical properties. Pharm Res. 2007;24:1118–30.
25. Martinez M, Amidon G. A mechanistic approach to understanding the factors affecting drug absorption: a review of fundamentals. J Clin Pharmacol. 2002;42:620–43.
26. Wu C, Benet L. Predicting drug disposition *via* application of BCS: transport/absorption/elimination interplay and development of a biopharmaceutics drug disposition classification system. Pharm Res. 2005;22:11–23.
27. Yu LX. An integrated model for determining causes of poor oral drug absorption. Pharm Res. 1999;16:1883–7.
28. Rudolph A, Tuthill C, inventors. Pharmaceutical formulations comprising substituted xanthine compounds. United States patent application 2006/0052404 A1.
29. Technical data on Pluronic(R) polyols. BASF Corporation.
30. Cohen J. Theophylline. Anal Profiles Drug Subst. 1975;4:466–93.
31. McPherson TB. Characterization of the aqueous solubility of CPX. AAPS Journal. 2006;8:T2278.
32. Stephenson G. Anisotropic lattice contraction in pharmaceuticals: the influence of cryo-crystallography on calculated powder diffraction patterns. J Pharm Sci. 2006;95:821–7.